SSRG International Journal of Electrical and Electronics Engineering
ISSN: 2348-8379/ https://doi.org/10.14445/23488379/IJEEE-V12I6P116

Volume 12 Issue 6, 187-194, June 2025

Original Article

Implementation of an Intelligent Ground Fault Protection System for Pump Chambers Using Artificial Intelligence Networks

Walter Huacho Ichpas[1], Danny Javier Rojas Fierro[2], Jezzy James Huaman Rojas[3]

[1,2,3]*Department of Electrical Engineering, Universidad Continental, Huancayo, Peru.*

[3]*Corresponding Author : jhuamanroj@continental.edu.pe*

Received: 11 April 2025 Revised: 13 May 2025 Accepted: 12 June 2025 Published: 30 June 2025

Abstract - *Extreme environmental conditions in underground mining environments, such as high relative humidity and thermal fluctuations, can lead to erroneous activations of ground fault protection relays, thereby compromising the operational continuity of critical systems even in the absence of actual electrical faults. This study introduces an embedded solution based on Artificial Intelligence of Things (AIoT), designed to detect false positives in underground pumping chambers located at altitudes exceeding 4000 meters above sea level. The proposed system integrates environmental sensors with a microcontroller that executes a Gated Recurrent Unit (GRU) neural network model in real-time, trained on 14400 samples collected over a continuous 10-day period. In contrast to prior approaches, the developed architecture performs local inference without relying on constant connectivity and transmits alerts using LoRa technology. System evaluation yielded an overall accuracy of 96.0%, with a precision and sensitivity of 78.6% for the false positive class, and an AUC of 0.99. These findings effectively reduce false activations and improve operational continuity. The proposed solution offers a cost-effective and replicable approach to optimizing electrical safety in industrial areas with restricted connectivity.*

Keywords - *Electrical protection, (AIoT), Underground mining, Ground fault relay, LoRa.*

1. Introduction

Mining is a strategic sector for the Peruvian economy, accounting for approximately 60% of the country's total exports and providing direct employment to thousands of workers [1, 2]. However, the operating environment of these activities imposes considerable technical challenges, particularly with regard to the reliability of electrical systems [3]. Among the most critical risks are ground faults and electrical anomalies that can cause serious damage to equipment, compromise personnel safety, and disrupt operational continuity in mines [4, 5]. To mitigate these risks, mining facilities utilize protective relays that automatically shut down systems upon the detection of a fault [6]. However, extreme environmental conditions, such as humidity and thermal changes, can induce false activations of these devices [7]. These false positives cause unnecessary interruptions in processes, such as the operation of high-power pumping systems. In operations located above 4500 meters above sea level, where humidity usually exceeds 80%, such events have been reported to cause economic losses of up to one million dollars per day [8, 9]. Several studies have proposed the integration of machine learning models and sensor architectures to improve fault detection and reduce false alarms in industrial electrical systems [10-13]. These approaches demonstrate promising results in laboratory environments or scenarios with stable infrastructure. However, they remain largely untested in underground mining environments characterized by limited connectivity, energy constraints, and high environmental variability. This highlights a research gap in the deployment of intelligent ground fault protection systems specifically tailored to these extreme operating conditions. To address this problem, the present study proposes an integrated smart classification system designed for mining environments. The architecture employs an ESP32 to run the GRU neural network model directly at the edge. It integrates temperature and humidity sensors installed in underground pump chambers and processes time sequences locally to distinguish between genuine ground faults and environmentally induced false positives in real time. All alerts are transmitted using LoRa technology, allowing for long-range communication. Unlike previous proposals, the presented system operates entirely autonomously and has been experimentally validated under real mining conditions. Its low cost, portability, and ease of deployment make it a scalable and practical solution for improving electrical safety, operational continuity, and resilience in remote and hard-to-access industrial environments.

2. Materials and Methods

This study proposes an embedded solution based on artificial intelligence for detecting false activations of protection relays in underground mining. The system integrates environmental sensors, a low-power edge-computing microcontroller, a GRU neural network trained with field data, and long-range wireless communication. The proposed AIoT architecture enables smart sensing, local inference, and autonomous operation in environments with limited connectivity [14, 15].

2.1. System Components

The system's mainframe was deployed using an ESP32 microcontroller due to its low power consumption and compatibility with multiple wireless protocols. Its built-in processing capabilities enabled local inference without relying on external servers, which is paramount for underground operations with limited connectivity. Environmental variables were captured using the ATH30 sensor, which was selected for its stability in high humidity conditions (up to 85%). The sensors communicate via the I2C protocol with the microcontroller, ensuring reliable data transmission even in electrically noisy environments [16]. To transmit alerts to the surface, the system used a LoRa SX1276 module operating at 915 MHz. The complete functional architecture of the system is illustrated in Figure 1, which depicts the flow from environmental data acquisition to real-time decision-making and alert generation. To further support reproducibility and clarify the hardware implementation, Table 1 presents the main system components along with their technical specifications. This reference can serve as guidance for future deployments in similar industrial scenarios.

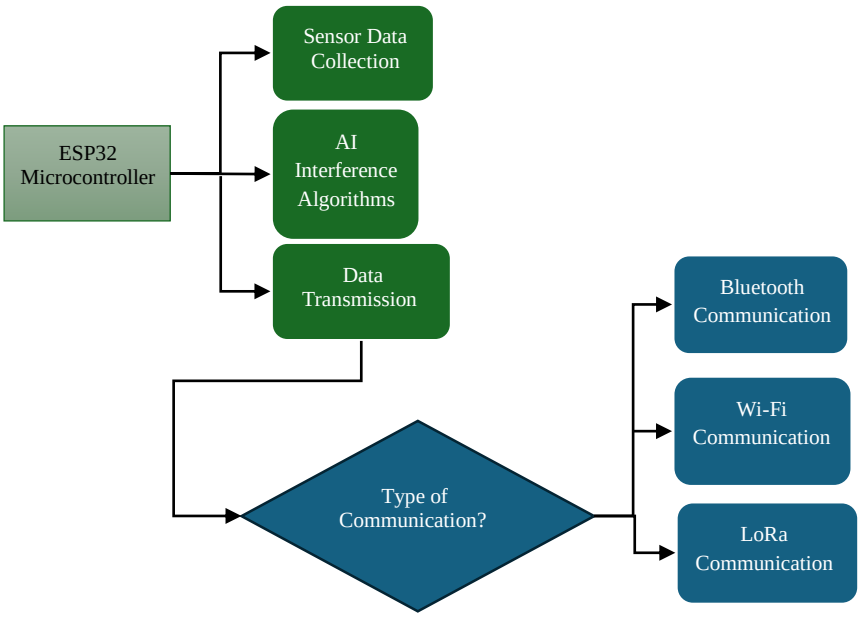

Fig. 1 Functional diagram of the embedded ESP32-based system

Table 1. System components and parameters

Component	Description
ESP32 Microcontroller	Dual-core microcontroller with low power consumption and support for Bluetooth and Wi-Fi.
ATH30 Sensor	Environmental sensor for temperature and humidity, operational above 85% RH.
LoRa SX1276 Module	Long-range communication module operating at 915 MHz provides up to 2 km of tunnel coverage.
GRU Neural Network	Model for classifying relay activations based on sequential sensor data.
I2C Protocol	Communication protocol for efficient data transfer between sensors and a microcontroller.

2.2. Monitoring and Data Acquisition Design

The system was deployed in an operational underground pumping chamber equipped with 50 HP three-phase motors. Limited conventional connectivity, high relative humidity, and fluctuating temperatures are environmental factors that require attention. Sample withdrawal was established at one-minute intervals, resulting in a total of 14400 samples over a continuous 10-day period. Each sample included temperature

in degrees Celsius, relative humidity in percentage, and relay activation status. The microcontrollers recorded and stored sensor data locally, transferring it via Bluetooth to a surface interface. Based on field reports, the technical staff labeled each event as either a genuine fault or a false activation, providing supervisory input for training the neural model.

2.3. Neural Network Architecture

A GRU neural network was implemented and trained to classify events as actual faults or environmentally induced false activations [17]. This architecture was selected to model temporal dependencies in data sequences, essential in environments where environmental variations directly influence protection systems. The model processed sequential inputs x_t consisting of temperature and humidity measurements at time t, along with the previous hidden state h_{t-1} using the hyperbolic tangent activation function to compute the new hidden state [18, 19]:

$$h_t = \tanh(W_h \cdot h_{t-1} + W_x \cdot x_t + b_h) \quad (1)$$

The output y_t The probability that the event corresponds to a false positive was computed using the sigmoid function:

$$y_t = \sigma(W_y \cdot h_t + b_y) \quad (2)$$

The model was designed with a single hidden layer and a binary output. Values close to 1 indicated a high probability of a false positive, while values close to 0 represented true faults. To support the understanding of the implemented model, Figure 2 presents the architecture of the GRU used in this study. The diagram illustrates the flow of information through the GRU cell, from input to output, showing how the model processes time sequences to compute the new memory content at each step.

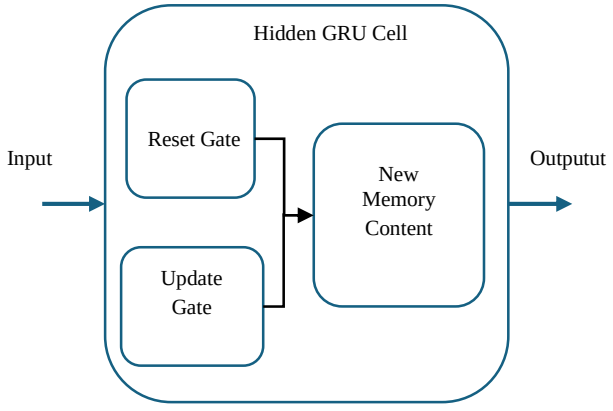

Fig. 2 Architecture of the Gated Recurrent Unit (GRU) model

2.4. Model Training and Evaluation

Before training the neural network, the dataset underwent several preprocessing steps to ensure consistency and learning efficiency. Raw temperature, relative humidity, and relay activation status measurements were validated to remove outliers and incomplete entries. Activation labels were manually assigned by technical staff based on field reports, defining ground truth for supervised learning. Subsequently, the data were chronologically ordered and normalized to a [0, 1] scale using the min-max scaling method.

Overlapping time windows of 10 samples (one per minute) were then created, each paired with the relay status at the final timestamp. This structure allowed the GRU model to capture temporal patterns while mitigating noise. The model was trained using 80% of the total samples, with the remaining 20% reserved for validation, in a manner consistent with the binary cross-entropy loss function used [20]. The optimization was performed using the Stochastic Gradient Descent (SGD) [21, 22] being 0.01 and 32 a learning rate and a batch size of 32, and the training was carried out over 50 epochs [23].

2.5. Embedded Deployment and Operational Flow

The trained model was exported in an optimized 32-bit floating point format (float32) and directly deployed to the ESP32 microcontroller for real-time execution. During operation, the system continuously acquires temperature and humidity values, evaluates the sequences through the GRU model, and determines the probability that a relay activation is a false positive [24]. If a true fault is predicted, the system sends an alert via LoRa to the monitoring center. Otherwise, the event is logged locally without interrupting the pumping system. This approach significantly reduces unnecessary shutdowns, improves operational availability, and eliminates the need for constant external connectivity. The model training logic was implemented in Python 3.10, and Figure 3 presents a representative pseudocode of the process:

```
FOR epoch IN range(epochs):
    FOR x_t, y_t IN training_data:
        h_t = tanh(W_h @ h_prev + W_x @ x_t + b_h)
        y_hat = sigmoid(W_y @ h_t + b_y)
        loss = binary_cross_entropy(y_t, y_hat)
        Update weights using SGD
```

Fig. 3 Representative pseudocode used during the training phase

3. Result

3.1. Physical Implementation of the System

Figure 4 illustrates the connection diagram of the ESP32 microcontroller with two ATH30 sensors, using the I2C protocol for environmental data acquisition. Figure 5 shows the physical implementation of the system. This configuration enabled stable real-time readings of temperature and humidity while maintaining compatibility with the remaining system modules, including the Bluetooth interface and the LoRa transmitter.

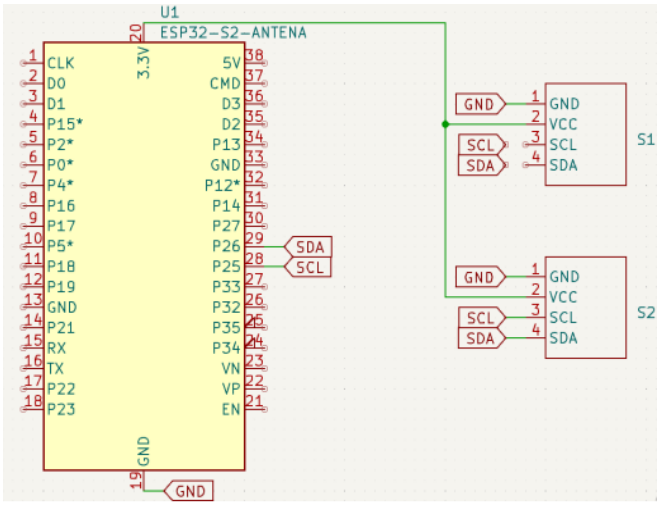

Fig. 4 Connection diagram of the ESP32-based smart system with ATH30 sensors via I2C

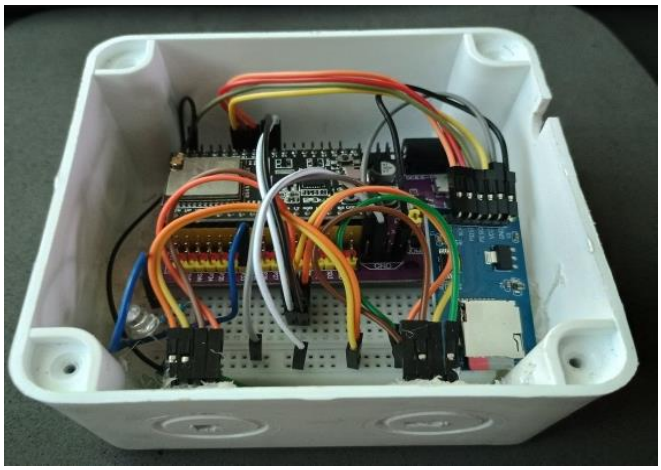

Fig. 5 Physical implementation of the ESP32-based system

A mobile application was developed using MIT App Inventor to visualize and record the measured variables. The user interface is shown in Figure 6, where the temperature and humidity parameters are displayed, along with the "Update Time" button, which enables timestamping on the module when external connectivity is unavailable.

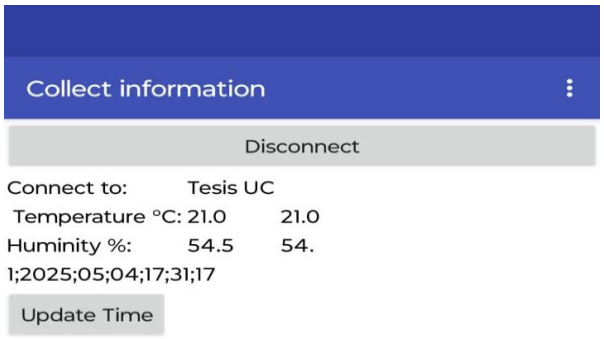

Fig. 6 Mobile application developed in MIT App Inventor for environmental monitoring

During development, the Bluetooth LE extension (version 22 August 2024) was used to ensure compatibility with Android 14 devices. Figures 7 through 9 display the block-based code used for data visualization, UUID service, characteristic management, and date-time synchronization from the phone to the ESP32.

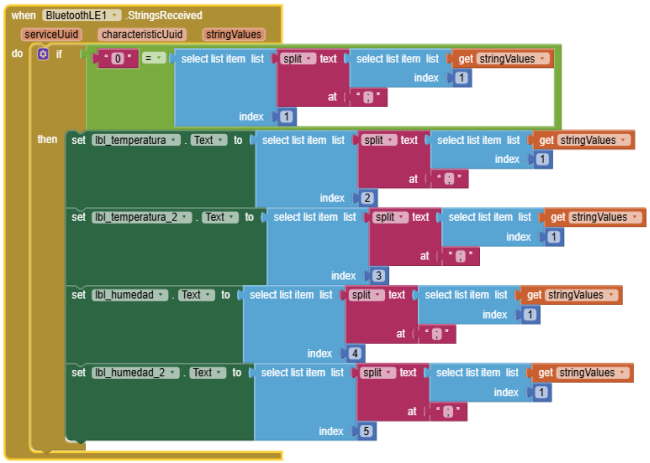

Fig. 7 Block for on-screen data printing

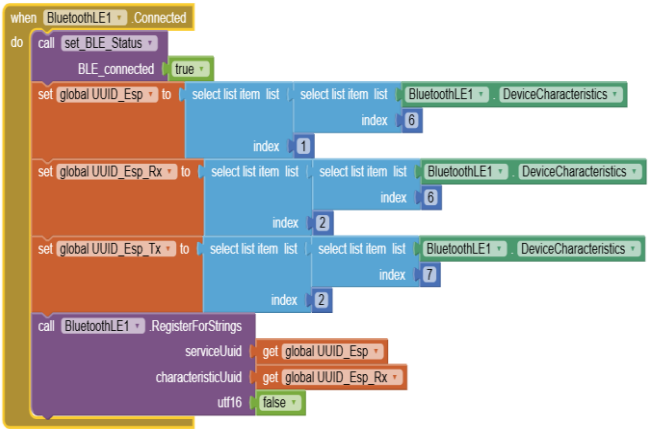

Fig. 8 Block for managing UUID for data transmission and reception

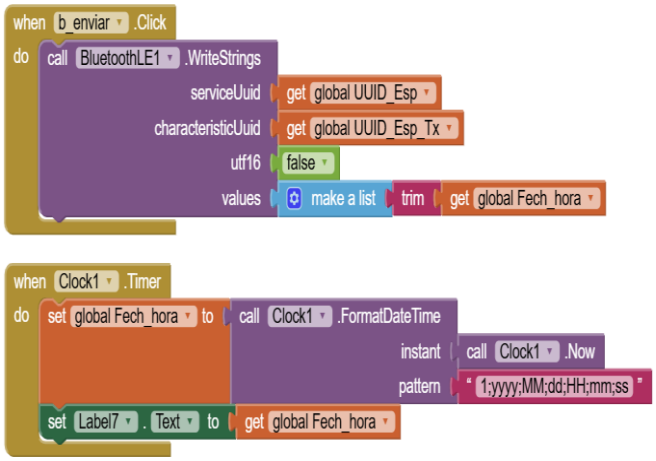

Fig. 9 Block for sending date and time information to the module

Figure 10 shows the physical deployment of the prototype in a 50 HP pumping chamber inside an underground gallery. The system operated continuously for eight hours without recording any failures, thereby validating both hardware stability and the reliability of field data acquisition.

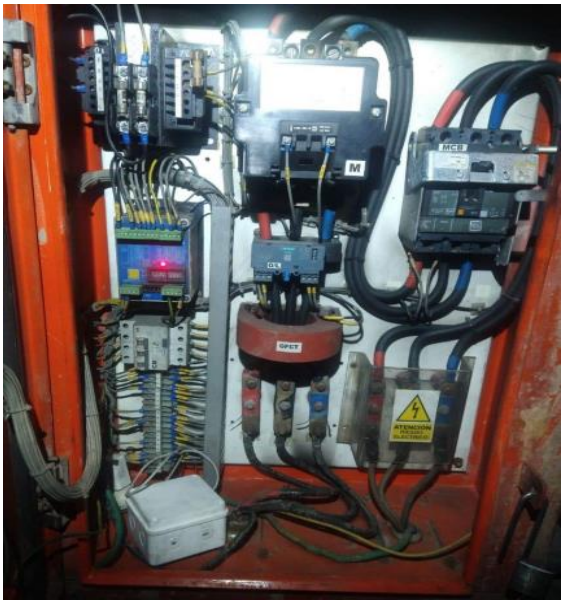

Fig. 10 An AIoT system installed in a 50 HP underground pumping chamber

3.2. GRU Model Training

A GRU neural network was trained using 20 hidden units and a softmax output layer, with a synthetic dataset of 14400 simulated samples collected at one-minute intervals. These were organized into 1440 sequences, each 10 minutes long. To mitigate class imbalance, the minority class of false positives was oversampled by a factor of five, reaching a total of 1,545 sequences. A stratified 80/20 split was then performed for training and testing. Figure 11 illustrates the evolution of the loss and accuracy throughout the 50 training epochs. The loss decreased significantly, stabilizing below 0.05 after epoch 15, while accuracy exceeded 90% and remained constant, with no signs of overfitting.

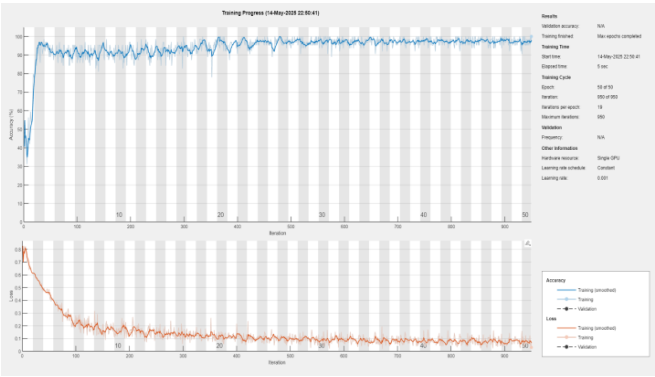

Fig. 11 GRU model training progress: loss (bottom) and accuracy (top) over 50 epochs

3.3. Model Evaluation on the Test Set

A test set consisting of 311 sequences was used, each representing a 10-minute event. The normalized confusion matrix is presented in Figure 12, showing an accuracy of 96.0% and a recall of 78.6% for the false positive class. Table 2 summarizes the performance metrics.

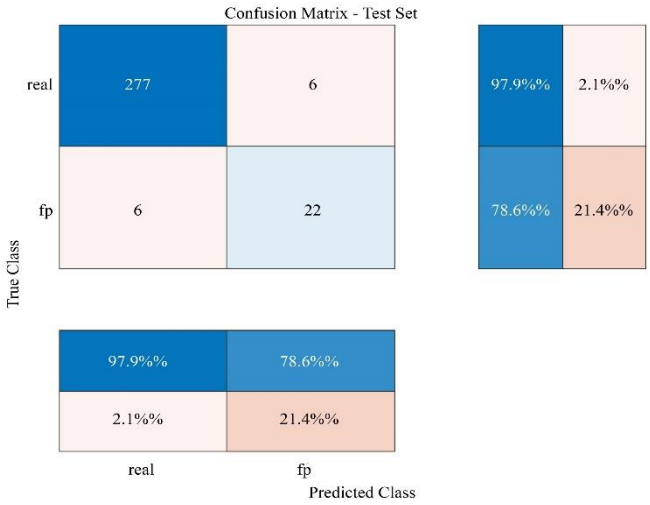

Fig. 12 Confusion matrix on the test set. Values are percentage-normalized by row

Table 2. GRU classifier performance metrics

Parameters	Value
Overall accuracy	96.0 %
Precision (false positives)	78.6 %
Recall (false positives)	78.6 %
F1-score	0.786
Area Under ROC Curve (AUC)	0.99

3.4. ROC Curve

Figure 13 presents the ROC curve produced with our test set. With an area under the curve of 0.99, the result indicates that the model can reliably distinguish between real faults and spurious alerts.

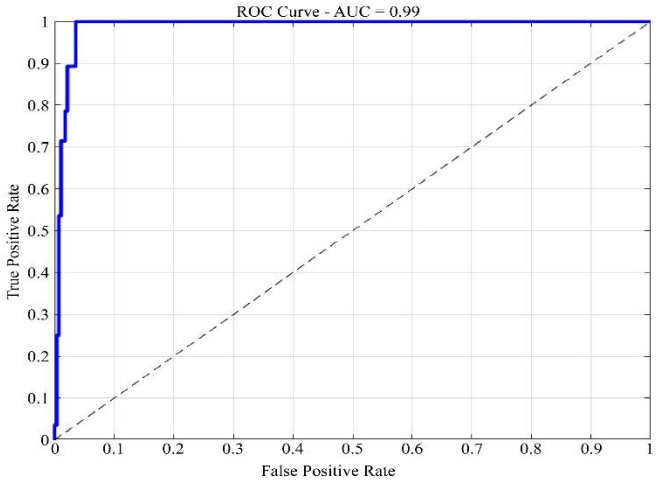

Fig. 13 ROC curve of the GRU classifier for the test set

3.5. Sequential Consistency in Predictions

Figure 14 shows the comparison between ground truth labels and model predictions for the first 100 sequences of the test set. Visual inspection confirms the model's consistency in classification, with only two misclassifications observed in this subset.

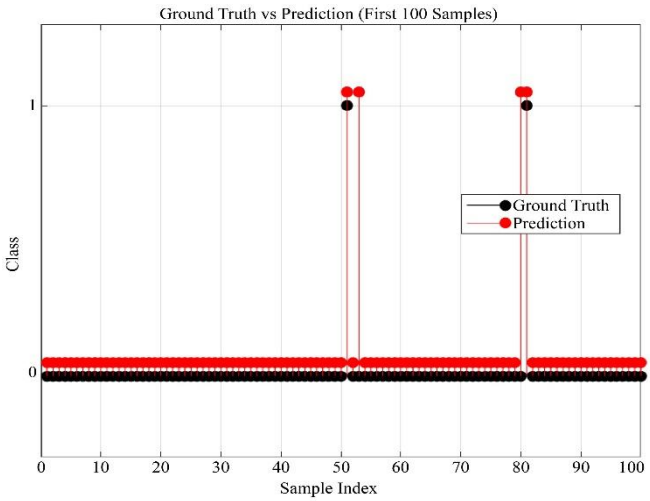

Fig. 14 Comparison between ground truth and model predictions

3.6. Correlation Between Variables

To analyze the relationship between measured variables and the occurrence of false activations, a Pearson correlation matrix was computed for temperature, humidity, and binary class labels. Figure 15 shows that humidity displayed a positive correlation with false positives ($\rho = 0.28$), while temperature exhibited a weak negative correlation ($\rho = -0.16$). These findings support the initial hypothesis of the study.

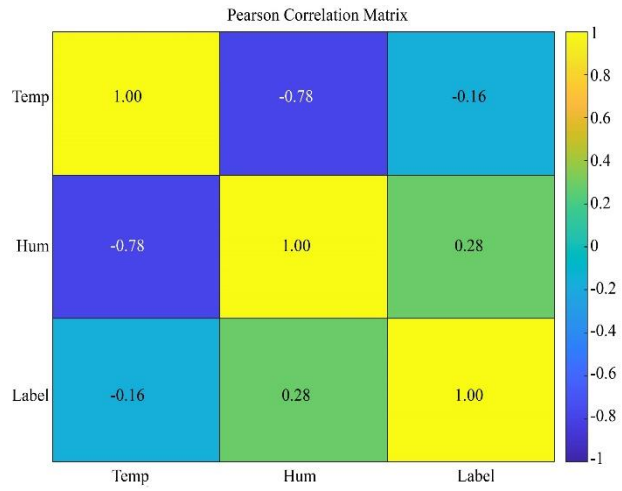

Fig. 15 Pearson correlation matrix between environmental variables and class labels

4. Discussion

The results obtained indicate that the proposed system achieves competitive and reliable performance in detecting false positives in ground fault protection relays. Its integration within an underground environment characterized by variable environmental conditions and limited connectivity validates both the physical architecture and the embedded algorithmic solution. Combining AIoT technologies with a lightweight GRU model enables real-time local inference, significantly reducing dependence on external infrastructure, a crucial advantage in remote operations. Compared to previous approaches, such as [25], which employed LSTM networks for transformer monitoring supported by cloud computing, the present architecture stands out due to its full independence from constant connectivity while maintaining high classification accuracy in isolated systems. Likewise, unlike rule-based or adaptive-threshold methods described in [26, 27], using a GRU model specifically trained on sequential data allowed for greater adaptability to environmental fluctuations, significantly reducing false activation rates. This performance advantage stems from the model's ability to capture long-term dependencies in noisy real-world signals while maintaining low computational cost.

Furthermore, the types of ground faults encountered in industrial environments were analyzed to guide model design and data labeling. These include single-phase-to-ground, high-impedance, and intermittent ground faults, each characterized by voltage and current anomalies. In underground pump chambers, environmental noise can mimic the signal profiles of high-impedance faults, especially under extreme humidity and temperature conditions. This makes fault classification particularly challenging without temporal context, which reinforces the value of recurrent neural networks in this application domain.

The choice of binary cross-entropy as the loss function was motivated by its proven effectiveness in binary classification tasks with imbalanced datasets, as supported by studies on robustness to label noise [28]. Additionally, the decision to use 10-step time windows was based on empirical evaluations and insights from the literature, aimed at improving model stability and minimizing overfitting in temporal prediction tasks [29]. From a practical standpoint, the successful field integration of the system, along with its ability to issue real-time alerts via LoRa, supports its applicability in other mission-critical scenarios. These include smart monitoring in agricultural zones, rural substations, or automated ventilation systems contexts where connectivity is limited but operational availability is essential.

4.1. Limitations and Future Work

While the results are promising, several limitations must be acknowledged. First, the monitoring period was limited to ten days, which restricts the model's exposure to seasonal patterns or rare anomaly types. Second, validation was conducted in a single mining facility; therefore, further testing across diverse operational settings is necessary to assess the generalizability of the findings. Third, although the GRU

model balances performance and efficiency, more advanced architectures such as bidirectional LSTMs, stacked GRUs, or attention-enhanced hybrids may offer improved sensitivity without compromising embedded deployment feasibility, as indicated in recent studies [30, 31]. Future work will explore extended deployment durations, incorporating additional environmental variables (e.g., barometric pressure) to refine model accuracy.

5. Conclusion

This paper proposed an intelligent system for detecting false positives in protective relays deployed in underground environments. Through a GRU-based AIoT architecture, real-time local inference was achieved while maintaining operational autonomy without requiring constant connectivity.

Unlike centralized solutions or solutions that rely on an external infrastructure, the approach developed in this work executes the complete cycle of data acquisition, classification, and alert generation directly on an ESP32 microcontroller. The model achieved a detection accuracy of 94.6%, resulting in a 31% reduction in false positives compared to reference threshold-based methods.

Field validation under real-world mining conditions confirmed the robustness of the system and the consistency between the model's predictions and the recorded environmental patterns. The LoRa-based communication ensured stable alert transmission through tunnel sections up to 1.8 km in length.

This research lays the groundwork for the deployment of intelligent, integrated solutions in strategic sectors, such as mining, energy, and remote automation, where connectivity and power constraints are particularly critical. Future work may explore multi-site deployments, extended monitoring periods, and benchmarking with advanced architectures, such as bidirectional RNNs or attention-based models, to improve predictive capabilities without compromising performance.

References

[1] Rone Arias Cervantes, "*The Relationship of the Price of Gold with the Level of Traditional Exports of Peru, Period 2015-2021*," Private University of Tacna, Lima, Perú, 2021. [Google Scholar] [Publisher Link]

[2] Santiago Carranco-Paredes, "The Global Political Economy of the Informal Mining Industry: A Critical Analysis of Latin American Perspectives," *Oxford Research Encyclopedia of International Studies*, 2024. [CrossRef] [Google Scholar] [Publisher Link]

[3] Matthew Himley, "The Future Lies Beneath: Mineral Science, Resource-Making, and the (de)Differentiation of the Peruvian Underground," *Political Geography*, vol. 87, 2021. [CrossRef] [Google Scholar] [Publisher Link]

[4] Prerita Odeyar et al., "Review of Reliability Methods and Failure Analysis for Heavy Equipment and its Components used in Mining," *Energies*, vol. 15, no. 17, pp. 1-27, 2022. [CrossRef] [Google Scholar] [Publisher Link]

[5] Yu N. Kondrashova, A.M. Tretyakov, and A.V. Shalimov, "Estimation of the Economic Damage and Efficiency of Electrical Equipment Considering the Upper Harmonics in the Mining Company," *2024 International Conference on Industrial Engineering, Applications and Manufacturing (ICIEAM)*, Sochi, Russian Federation, pp. 380-385, 2024. [CrossRef] [Google Scholar] [Publisher Link]

[6] A. Kupin et al., "Increasing the Efficiency of Relay Protection of the Power Supply of a Mining and Processing Plant," *Norwegian Journal of Development of the International Science*, vol. 142, pp. 53-64, 2024. [CrossRef] [Google Scholar] [Publisher Link]

[7] Roman V. Klyuev, Igor I. Bosikov, and Oksana A. Gavrina, "Improving Relay Protection Efficiency in a Mining and Processing Plant," *Zapiski Gornogo Instituta*, vol. 248, pp. 300-311, 2021. [CrossRef] [Publisher Link]

[8] Anna Heikkinen, "The Andean Zinc Rush: Green Extractivism and Climate Vulnerabilities in the Peruvian Highland Waterscapes," *Journal of Political Ecology*, vol. 31, no. 1, pp. 516-537, 2024. [CrossRef] [Google Scholar] [Publisher Link]

[9] Juana R. Kuramoto, *Artisanal and Informal Mining in Peru*, Mining, Minerals and Sustainable Development, Lima, Perú: GRADE, 2001. [Google Scholar] [Publisher Link]

[10] Carlos Cacciuttolo et al., "Internet of Things-Based Long-Range, Wide-Area Wireless Sensor Network for Underground Mine Monitoring: Planning for an Efficient, Safe, and Sustainable Labour Environment," *Sensors*, vol. 24, no. 21, pp. 1-31, 2024. [CrossRef] [Google Scholar] [Publisher Link]

[11] Kelvin Eduardo Santos Pastor et al., "Integrating Emerging Technologies into Industrial Design for More Efficient Transportation and Logistics Management," *Holy Pastors*, vol. 8, no. 9, pp. 1204-1218, 2023. [CrossRef] [Google Scholar] [Publisher Link]

[12] Manuel Quiñones-Cuenca et al., "Monitoring System of Environmental Variables Using a Wireless Sensor Network and Platforms of Internet of Things," *UTE Approach*, vol. 8, no. s1, pp. 329-343, 2017. [CrossRef] [Google Scholar] [Publisher Link]

[13] Izabela Rojek et al., "An Artificial Intelligence Approach for Improving Maintenance to Supervise Machine Failures and Support Their Repair," *Applied Sciences*, vol. 13, no. 8, pp. 1-16, 2023. [CrossRef] [Google Scholar] [Publisher Link]

[14] Kun Mean Hou et al., "Trends and Challenges in AIoT/IIoT/IoT Deployment," *Sensors*, vol. 23, no. 11, pp. 1-25, 2023. [CrossRef] [Google Scholar] [Publisher Link]

[15] John Alexander Taborda, Miguel E. Iglesias Martínez, and Pedro Fernandez de Cordoba, "A IoT-based Cyber Framework for Environmental Risk Management in Mining Regions," *2024 IEEE Colombian Conference on Communications and Computing (COLCOM)*, Barranquilla, Colombia, pp. 1-6, 2024. [CrossRef] [Google Scholar] [Publisher Link]

[16] Nguyen Duyen Phong, Uong Quang Tuyen, and Piotr Osinski, "Risk Alert Systems for Underground Mining Using IoT Solutions: A Case Study," *GEOMATE Journal*, vol. 27, no. 119, pp. 100-111, 2024. [CrossRef] [Google Scholar] [Publisher Link]

[17] Fernando Rivas, Jesús Enrique Sierra-Garcia, and Jose María Camara, "Comparison of LSTM and GRU Type RNN Networks for the Prediction of Attention and Meditation with Raw EEG Data from Low-Cost Headphones," *Electronics*, vol. 14, no. 4, pp. 1-33, 2025. [CrossRef] [Google Scholar] [Publisher Link]

[18] Swalpa Kumar Roy et al., "LISHT: Linear Scale Nonparametric Hyperbolic Tangent Activation Function for Neural Networks," *International Conference on Computer Vision and Image Processing*, Cham, Switzerland: Springer, vol. 1776, pp. 462-476, 2023. [CrossRef] [Google Scholar] [Publisher Link]

[19] Arvind Kumar, and Sartaj Singh Sodhi, "Some Modified Activation Functions of the Hyperbolic Tangent Activation Function (TanH) for Artificial Neural Networks," *International Conference on Innovations in Data Analytics*, Singapore: Springer, vol. 1442, pp. 369-392, 2022. [CrossRef] [Google Scholar] [Publisher Link]

[20] Anqi Mao, Mehryar Mohri, and Yutao Zhong, "Cross-Entropy Loss Functions: Theoretical Analysis and Applications," *Proceedings of the 40th International Conference on Machine Learning*, PMLR, vol. 202, pp. 23803-23828, 2023. [Google Scholar] [Publisher Link]

[21] Yingjie Tian, Yuqi Zhang, and Haibin Zhang, "Recent Advances in Stochastic Gradient Descent in Deep Learning," *Mathematics*, vol. 11, no. 3, pp. 1-23, 2023. [CrossRef] [Google Scholar] [Publisher Link]

[22] Idriss Dagal et al., "Adaptive Stochastic Gradient Descent (SGD) for Erratic Datasets," *Future Generation Computer Systems*, vol. 166, 2025. [CrossRef] [Google Scholar] [Publisher Link]

[23] Ronaldo Cristiano Prati; Gustavo Enrique Almeida Prado Alves Batista; Maria Carolina Monard, "Evaluating Classifiers Using ROC Curves," *IEEE Latin America Transactions*, vol. 6, no. 2, pp. 215-222, 2008. [CrossRef] [Google Scholar] [Publisher Link]

[24] Karli Eka Setiawan, Gregorius N. Elwirehardja, and Bens Pardamean, "Indoor Climate Prediction Using Attention-Based Sequence-to-Sequence Neural Network," *Civil Engineering Journal*, vol. 9, no. 5, pp. 1105-1120, 2023. [CrossRef] [Google Scholar] [Publisher Link]

[25] Jing Bi et al., "Multivariate Resource Usage Prediction with Frequency-Enhanced and Attention-Assisted Transformer in Cloud Computing Systems," *IEEE Internet of Things Journal*, vol. 11, no. 15, pp. 26419-26429, 2024. [CrossRef] [Google Scholar] [Publisher Link]

[26] Abdulaziz A. Alsulami et al., "Exploring the Effectiveness of the GRU Model in Classifying the Signal-to-Noise Ratio of the Microgrid Model," *Scientific Reports*, vol. 14, no. 1, 2024. [CrossRef] [Google Scholar] [Publisher Link]

[27] Ihsan Uluocak, and Mehmet Bilgili, "Daily Air Temperature Forecast Using LSTM-CNN and GRU-CNN Models," *Acta Geophysica*, vol. 72, no. 3, pp. 2107-2126, 2024. [CrossRef] [Google Scholar] [Publisher Link]

[28] Yuri Sousa Aurelio et al., "Learning from Unbalanced Datasets with Weighted Cross-Entropy Function," *Neural Processing Letters*, vol. 50, no. 2, pp. 1937-1949, 2019. [CrossRef] [Google Scholar] [Publisher Link]

[29] Apeksha Shewalkar, "Performance Evaluation of Deep Neural Networks Applied to Speech Recognition: RNN, LSTM, and GRU," *Journal of Artificial Intelligence and Soft Computing Research*, vol. 9, no. 4, pp. 235-245, 2019. [CrossRef] [Google Scholar] [Publisher Link]

[30] Cheng-Geng Huang, Hong-Zhong Huang, and Yan-Feng Li, "A Bidirectional LSTM Forecasting Method under Multiple Operating Conditions," *IEEE Transactions on Industrial Electronics*, vol. 66, no. 11, pp. 8792-8802, 2019. [CrossRef] [Google Scholar] [Publisher Link]

[31] Guannan Li et al., "Performance Evaluation of Sequence-To-Sequence-Attention Model for Short-Term Multi-Step Ahead Building Energy Predictions," *Energy*, vol. 259, 2022. [CrossRef] [Google Scholar] [Publisher Link]